

Local and global order in a simulated two-dimensional liquid under steady shear

Scott Butler and Peter Harrowell

School of Chemistry, University of Sydney, Sydney, New South Wales 2006, Australia

(Received 26 January 1996)

The dependence of “stringlike” order on system size in nonequilibrium molecular dynamics simulations of a two-dimensional liquid of soft disks under steady shear is reported. Local order, as measured by the calculated Bragg intensities from a fixed scattering volume, is found to be independent of the simulation box length. The global ordering of the “strings,” however, is observed to decrease steadily with increasing cell length along the flow direction. This is a consequence of the increase in the number of uncorrelated domains as the system becomes larger. The implications of the (probable) disappearance of global order in the thermodynamic limit for the discussion concerning choice of thermostat is considered. It is suggested that the domains of shear-induced order may arise from the large structural fluctuations at equilibrium. [S1063-651X(96)02607-4]

PACS number(s): 61.20.Ja, 83.20.Hn, 83.20.Jp

I. INTRODUCTION

The development of molecular dynamics simulation methods for nonequilibrium steady states of liquids [1] marks an important advance in our understanding of dynamics in dense phases. This importance prompts us to examine carefully the remaining questions concerning the technique. One open question is the physical relevance of the results of simulations of ordered phases undergoing shear flow. This issue, in the context of shear induced order, has also become entangled with the question of the “correctness” of the various thermostats. We recently [2] identified a significant system size dependency of the shear induced disordering transition in a colloidal crystal. This was interpreted as arising from the strong coupling between the applied shear flow and the long wavelength transverse fluctuations of the shearing crystal. The general implication is that long wavelength fluctuations play a more significant role in determining nonequilibrium steady states than they do in stabilizing the equilibrium state. The finite system size and the periodic boundary conditions have also been shown [3] to stabilize shear induced structures observed in simulations of a colloidal suspension at high steady shear rates. In this paper we examine this finite size effect in the case of a soft disk liquid in two dimensions (2D) undergoing shear flow.

The question of the physical relevance of the shear induced ordering (SIO) in liquids under steady shear has prompted some discussion in the literature. The physical reality of this order was first called into question in 1986 by Evans and Morriss [4] who claimed that the ordered state they observed in nonequilibrium molecular dynamics (NEMD) calculations of a 2D liquid was an artifact of the profile-biased thermostat (PBT) used to remove the heat generated by shearing. Evans and Morriss observed the shear-induced order to disappear when a profile unbiased thermostat (PUT) was used. By concluding that the shear-induced ordering was the result of a simplistic thermostat, these authors linked the appearance of the shear-induced structure with a criterion for judging the “correctness” of a given thermostat. This issue, however, remains open. Other groups [5,6] have observed the persistence of shear-induced ordering using partially unbiased thermostats. Shear-induced or-

dering has been observed not only for NEMD algorithms but also in simulations which used nonequilibrium Brownian dynamics [3,7]. While these simulations do not have an explicit thermostat, the assumption of a linear velocity field in the solvent imposes a constraint similar to that of the profile biased thermostat. Shear-induced ordering has also been observed in Stokesian dynamics [8–10], which relaxes this assumption concerning the solvent velocity field and incorporates hydrodynamic interactions between colloidal particles.

In this paper we pursue the possibility that shear-induced ordering stems, not from the choice of the thermostat, but rather from the use of finite systems. To test for this we have carried out a series of NEMD simulations of a soft disk liquid in 2D and examined the dependence of the shear-induced structure on the length of the simulation cell in the velocity direction. (In our previous study [3] this was the only direction in which system size dependence was evident.) The use of a 2D system makes possible the investigation of a larger range of system sizes than in 3D for the testing of a dependence on system size.

II. BACKGROUND

As mentioned above shear-induced ordering has been observed in simulations of liquids under steady shear using NEMD [5,6,11,12], nonequilibrium Brownian dynamics [7] and Stokesian dynamics [8–10]. In 2D simulations [8,9] the ordered state is comprised of strings of particles aligned with the shear, the imposed velocity gradient forcing the strings to slide past one another. In 3D the ordered state is usually strings of particles aligned with the flow, these strings being hexagonally packed in the gradient-vorticity plane. (We note here for clarification that in this paper we address the issue of steady shear only. Shear-induced order is well established for oscillatory shear in both experiments [13] and simulations [13,14].)

Discussion about the reality of shear-induced ordering has primarily been concerned with thermostatting in NEMD systems. A thermostat is required in NEMD to remove heat generated by the applied shear. Without some mechanism for heat dissipation the shearing system would continually heat up, never reaching a steady state. The basic problem of ther-

mostating lies in dividing the momentum of a particle into two components: *streaming* and *peculiar*, with only the latter motion thermostated.

The simplest choice of thermostat has been labeled the profile-biased thermostat (PBT). This thermostat assumes that the streaming component of a particle's motion is that given by the linear velocity gradient set by the applied shear rate $\dot{\gamma}$. The validity of the PBT has, however, been called into question by Evans and Morriss [4]. Their objection is that the definition of streaming motion in the PBT restricts the dynamics of particles in an unphysical way. They argue that, while the boundaries of a shearing simulation are forced to shear a distance $\dot{\gamma}Lt$ in time t , where L is the height of the cell, it is not required that the velocity profile across the cell be linear. The PBT, however, defines the streaming motion to be perpendicular to the shear gradient and to have a linear velocity profile. This definition does not allow for structures such as convective rolls in which the streaming motion is not directed with the shear, or plug flow, in which the velocity profile is nonlinear. Evans and Morriss [4] argued that it was these restrictions that caused the high-shear-rate ordering observed using a PBT. (While not offering an explicit connection between the PBT and the ordering, these authors note [1] that the PBT will result in the generation of an additional contribution to the shear stress.)

To overcome the shortcomings of a PBT, Evans and Morriss implemented a profile-unbiased thermostat (PUT) in 2D simulations of soft discs [4]. Their PUT averaged over small cells of particles to determine a *local* streaming velocity which was subtracted from the motion of the particles in that cell to determine the peculiar component of the particles' motion. This peculiar motion was then thermostated. Evans and Morriss observed that the shear-induced ordering they had found using a PBT vanished when a PUT was used. In a similar vein, Evans and Morriss also implemented a PUT in a 3D simulation in which high-wave-vector components of the velocity space were thermostated [15]. No SIO was observed using this thermostat. Stevens, Robbins, and Belak [5] and Hess and Loose [6] have implemented partially unbiased thermostats in 3D systems in which the streaming motion of particles is calculated by averaging over layers of particles perpendicular to the shear gradient. Using such a PUT they do see shear-induced ordering. We note in passing that regardless of the type of thermostat used, the use of Lees-Edwards boundary conditions sets a linear velocity profile in the sliding image cells which has a coarse-grained effect similar to a PBT.

III. SIMULATION DETAILS

Avoiding the problems of boundary-driven systems requires a homogeneous algorithm for the propagation of particles which incorporates a shear flow. One such formalism is the Sllod equations of motion [defined below in Eqs. (1)–(3)] for the planar Couette flow [16], which include the shearing motion as an external field coupled to the equations of motion of the particles. These equations of motion, in conjunction with Lees-Edwards boundary conditions [17], give an exact description of adiabatic (i.e., unthermostated) planar Couette flow arbitrarily far from equilibrium.

The Sllod equations of motion, incorporating a Gaussian [18,19] PBT, are

$$\dot{\mathbf{q}}_i = \frac{\mathbf{p}_i}{m} + \dot{\gamma} \mathbf{i} q_{yi}, \quad (1)$$

$$\dot{\mathbf{p}}_i = \mathbf{F}_i - \dot{\gamma} \mathbf{i} p_{yi} - \alpha \mathbf{p}_i, \quad (2)$$

where

$$\alpha = \frac{\sum_i \mathbf{p}_i \cdot \mathbf{F}_i - \dot{\gamma} \sum_i p_{xi} p_{yi}}{\sum_i p_i^2}. \quad (3)$$

In these equations $\dot{\gamma}$ is the shear rate, \mathbf{i} is a unit vector in the x direction, m is the mass of a particle (reduced to $m=1$ in our work), \mathbf{p}_i refers to the *peculiar* momenta of the particles, and α serves to keep the kinetic temperature constant. At zero shear these equations reduce to Newton's equations of motion. In our simulations the Sllod equations were integrated numerically using a fifth-order Gear predictor-corrector method in conjunction with Lees-Edwards [17] "sliding-brick" boundary conditions.

We used a repulsive interparticle potential of the form

$$u(r) = \varepsilon (\sigma/r)^{12}, \quad (4)$$

where r is the distance between particles and ε and σ have units of energy and length, respectively. We use the following reduced units throughout this paper $\rho^* = \rho \sigma^2$, $r^* = r/\sigma$, $T^* = k_B T/\varepsilon$, and $\Delta t^* = \Delta t (\varepsilon/m\sigma^2)^{-1/2}$. A rectangular simulation cell was used for the 2D calculations. The cell dimensions L_x and L_y are given by

$$L_x = N_x \left(\frac{2}{\sqrt{3}\rho} \right)^{1/2},$$

$$L_y = N_y \left(\frac{\sqrt{3}}{2\rho} \right)^{1/2}, \quad (5)$$

where ρ is the density. These dimensions were chosen so as to accommodate a hexagonal structure aligned such that a perpendicular bisector of the triangular lattice is parallel to the y axis. N_x is the number of particles aligned along the x direction in each "string" of the hexagonal structure and N_y is the number of such strings. We will refer to cell dimensions in terms of the parameters N_x and N_y .

IV. RESULTS

A. Shear thinning and shear induced "strings"

Recent large scale simulations [20] indicate that the 2D r^{-12} system undergoes a continuous transition from the liquid to the hexatic phase at $\rho^*=1.000$ along the $T^*=1.00$ isotherm. We chose one equilibrium phase point ($T^*=1.00$, $\rho^*=0.95$) which has an amorphous structure and studied its properties under shear.

To probe the amount of stringlike order we calculated the intensity of Bragg scattering for wave vectors aligned in the gradient direction. The scattered intensity at wave-vector \mathbf{k} was calculated using

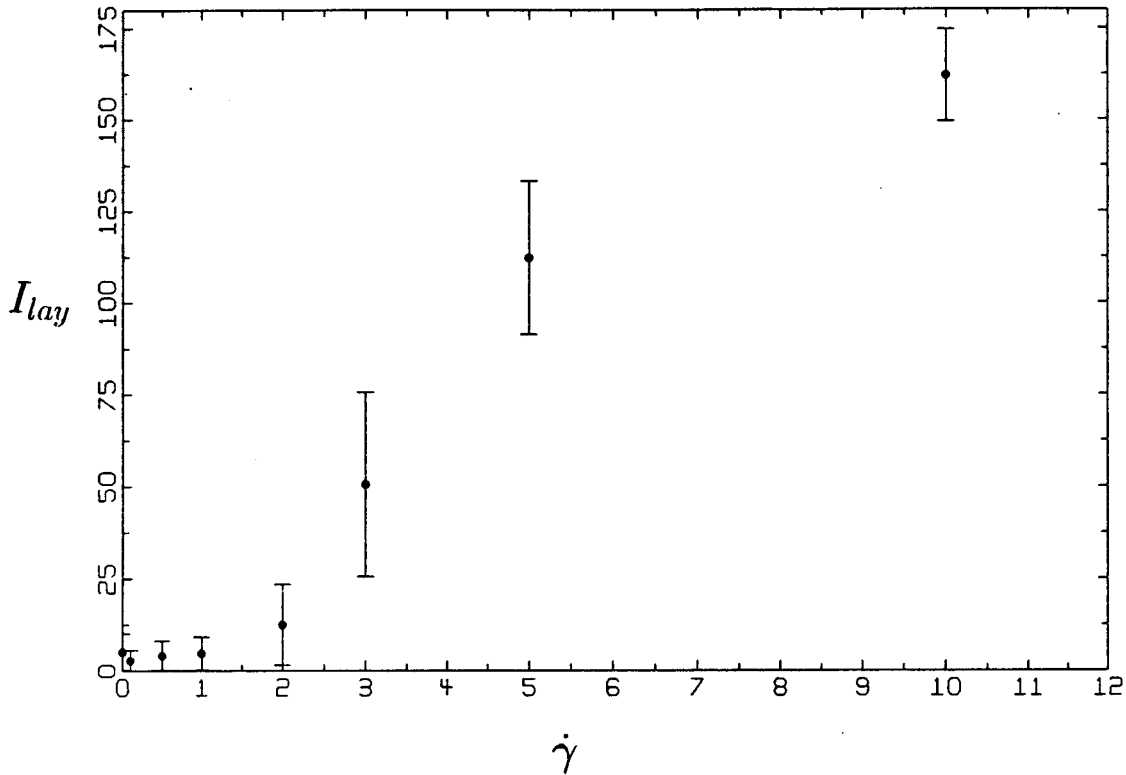


FIG. 1. The scattering intensity I_{lay} vs shear rate (in inverse number of time steps) for a liquid of 256 soft disks at $T^*=1.00$ and $\rho^*=0.95$. Note the continuous increase in shear induced structure.

$$I(\mathbf{k}) = 1 + \frac{2}{N} \sum_{i>j} \cos(\mathbf{k} \cdot \mathbf{r}_{ij}). \quad (6)$$

The wave vector for Bragg scattering from string structures is

$$\mathbf{k} = \left(0, \left(\frac{8\rho}{\sqrt{3}} \right)^{1/2}, \pi \right). \quad (7)$$

The scattered intensity at this wave vector will be referred to as I_{lay} . In addition, the shear stress was monitored, the stress σ_{xy} being calculated using

$$\sigma_{xy} = -V^{-1} \left\langle \sum_{i>j} y_{ij} F_{xij} \right\rangle, \quad (8)$$

where F_{xij} is the x component of the force between particles i and j , y_{ij} is the y displacement between particles i and j , V is the system volume, and $\langle \dots \rangle$ denotes a time average.

First, we characterized the steady-state structure under shear over a range of shear rates for systems of 256 particles at the chosen temperature and density, $T^*=1.00$, $\rho^*=0.95$. These calculations used $(N_x, N_y) = (16, 16)$, with a time step of $\Delta t^*=0.005$ for $\dot{\gamma} \leq 1$ and $\Delta t^*=0.002$ for $\dot{\gamma} > 1$. Figure 1 gives the shear-rate dependence of I_{lay} for the 256 particle system. The intensity of Bragg scattering changes little for shear rates up to $\dot{\gamma}=1$ but increases markedly between $\dot{\gamma}=1$ and $\dot{\gamma}=2$. The Bragg intensity increases monotonically with an increasing shear rate beyond $\dot{\gamma}=2$. The structural change occurring between $\dot{\gamma}=1$ and $\dot{\gamma}=2$ is accompanied by shear thinning as shown in Fig. 2. The stress increases rapidly on

application of a shear, reaching a constant value at $\dot{\gamma}=2$. Apart from the appearance of “stringlike” correlations evident in the scattering I_{lay} , we find no other structure. These correlations can be seen in sample particle configurations presented in Fig. 3 for shear rates at $\dot{\gamma}=1, 2$, and 3.

B. Dependence on system size

The primary motive of our study was to see if the non-equilibrium structure exhibited a dependence on system size, in particular, the cell dimension in the velocity direction. To test for this we fixed the density, shear rate, and y dimension of the cell and examined the dependence on x cell dimension of I_{lay} , the shear stress and the coherence of the shear-induced string structures. A shear rate of $\dot{\gamma}=2$ was chosen for this study, it being the shear rate at which the first definite increase in I_{lay} occurred and the shear stress had reached a constant value. The y dimension was set $N_y=16$ while the x dimension was varied over the range $N_x=8-120$, corresponding to particle numbers ranging from 128 to 1920.

We first consider the effect of extending the simulation cell on the shear stress and the scattering intensity I_{lay} . For each system size the shear was applied to an equilibrium liquid configuration and was run for 2×10^5 time steps to achieve a steady state. Stress and scattering averages were calculated over the subsequent 2×10^5 time steps. Shown in Fig. 4, the shear stress varies little as the x dimension is increased. The size dependence of I_{lay} is presented in Fig. 5. As the scattering intensity is only comparable for identical scattering volumes, a scattering volume of $8a \times 8a$ was used for each system, where a is the average interparticle distance. Other than a reduction in error with increasing system

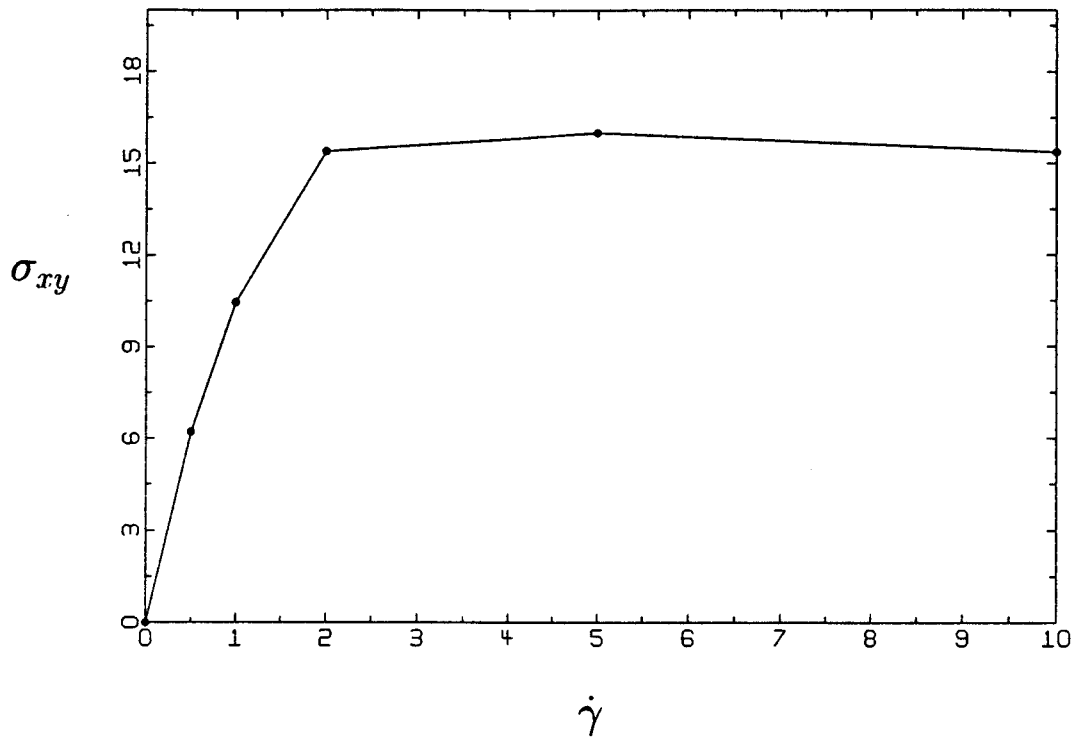


FIG. 2. Shear stress vs shear rate (in inverse number of time steps) for a liquid of 256 soft disks at $T^*=1.00$ and $\rho^*=0.95$. A substantial shear thinning is observed for $1 < \dot{\gamma} < 2$.

size, most likely due to better statistics in the larger systems, there is no discernible change in I_{1ay} as the x cell dimension is increased.

The scattering intensity reflects the degree of correlation between particle pairs under the imposition of the shear flow. Structure can also be defined in terms of the *single* particle

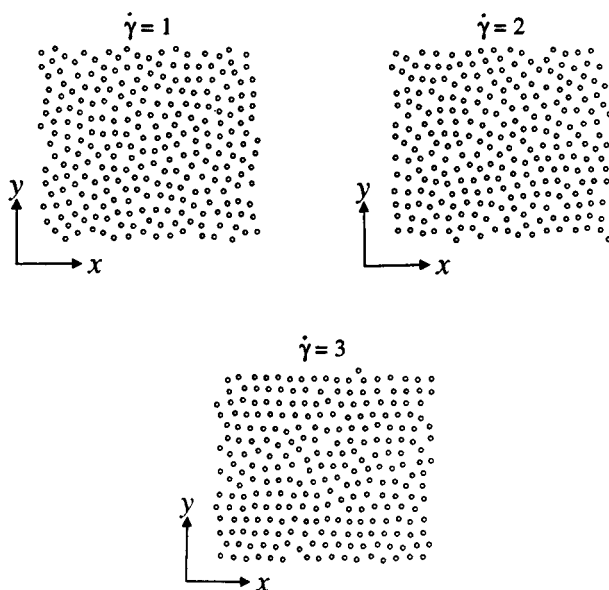


FIG. 3. Instantaneous particle configurations for an $(N_x, N_y) = (16, 16)$ system under shear at $T^*=1.00$ and $\rho^*=0.95$. Three different shear rates are shown with clear string correlations evident at $\dot{\gamma}=3$.

distribution. Here we consider the average projection of particle configurations onto the gradient direction as measured by $P(y)$, the probability of a particle being found at a ‘‘height’’ y in the cell. Figure 6 gives the function $P(y)$ at $\dot{\gamma}=2$ for systems of constant y dimension $N_y=16$ and x cell dimensions of $N_x=30, 50, 80$, and 120. The density profiles in Fig. 6 were averaged over 10 configurations, one taken every 50 time steps for 500 time steps. For all x dimensions studied, there are obvious density oscillations indicative of structure coherent over the x dimension of the cell. We also find that the amplitude of these density waves diminishes with increasing cell length. To measure the amplitude of the

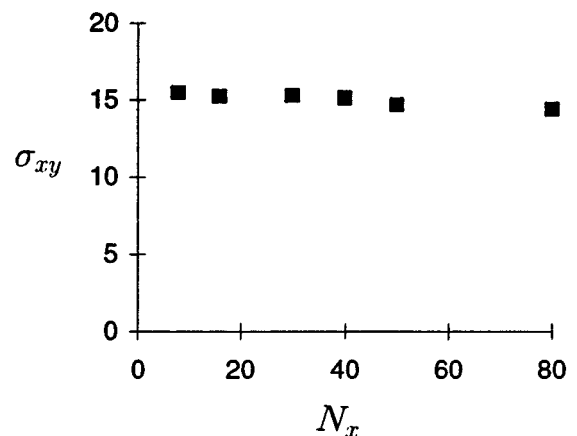


FIG. 4. The dependence of the shear stress at $\dot{\gamma}=2$ and $\rho^*=0.95$ on the cell dimension N_x .

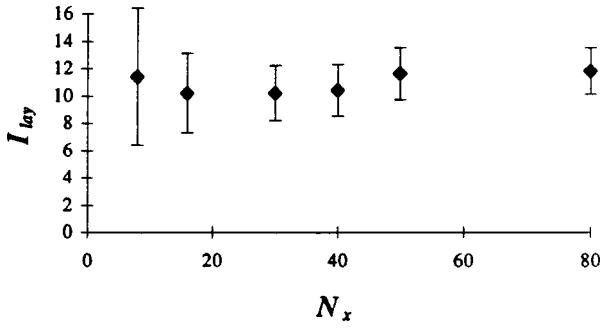


FIG. 5. The dependence of the scattering intensity I_{lay} on cell dimension in the flow direction, N_x , at $\dot{\gamma}=2$ and $\rho^*=0.95$. I_{lay} was calculated over an $8a \times 8a$ scattering volume for all system sizes studied.

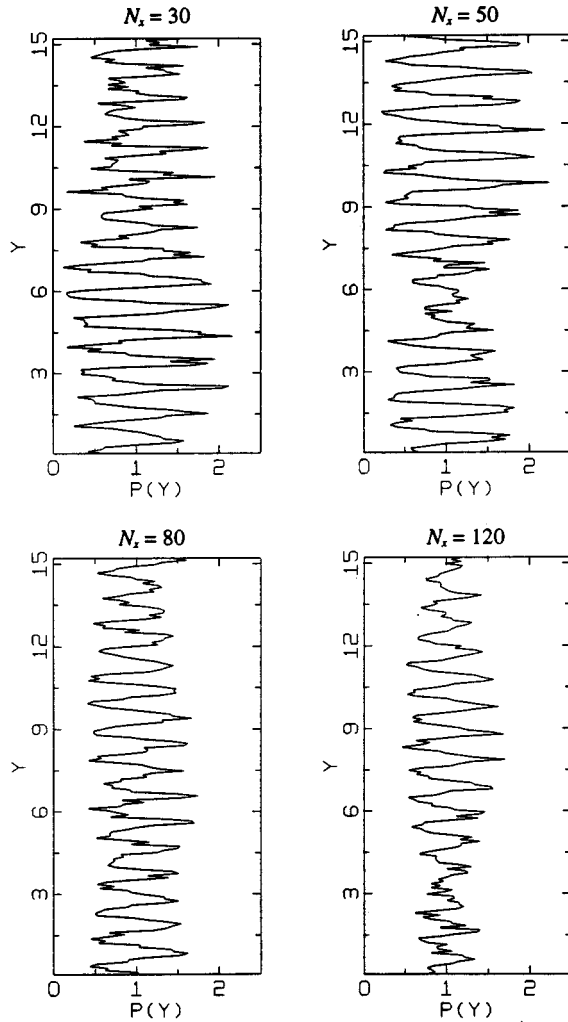


FIG. 6. The projection $P(y)$ of the density onto the y axis for systems at $\dot{\gamma}=2$, $T^*=1.00$, $\rho^*=0.95$ and with cell lengths $N_x=30$, 50, 80, and 120. Note the decrease in amplitude and coherence of density oscillations with increasing length along the direction of flow.

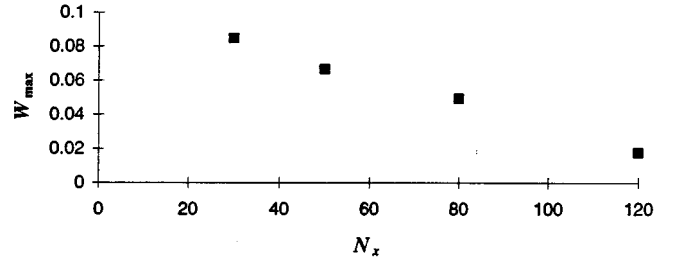


FIG. 7. The global order parameter W_{max} vs N_x for systems at $\dot{\gamma}=2$ and dimensions $N_x=30, 50, 80$, and 120 and $N_y=16$. Note the steady decrease of W_{max} with increasing cell length along the direction of flow.

density oscillations along the gradient coordinate we calculated the following Fourier transform:

$$W(q) = \frac{1}{L_y^2} \int_0^L \int_0^L [P(y_1) - \langle P \rangle][P(y_2) - \langle P \rangle] \times \cos[q(y_1 - y_2)] dy_1 dy_2, \quad (9)$$

where $\langle P \rangle$ is the average value of $P(y)$ for the system and L_y is the dimension of the cell along the shear gradient direction. We define an order parameter W_{max} as the maximum value of $W(q)$ over the space of q . The dependence of W_{max} on the x cell dimension, presented in Fig. 7, clearly shows a steady decrease in the value of W_{max} as the simulation cell is extended along the velocity direction.

How is that the W_{max} can decrease with increasing system size while the scattering intensity I_{lay} shows no such dependence? The answer lies in the spatial extent of the two measures of order. I_{lay} refers to the stringlike character within a scattering volume of $8a \times 8a$ while W_{max} measures the degree of stringlike ordering which spans the entire simulation cell. What we are seeing in our simulations are *patches* of locally correlated strings whose stability is unaffected by the finite nature of the simulation cell (at least over the values of T^* , ρ^* , and $\dot{\gamma}$ included in this study). The patches, however, are only weakly correlated with one another, hence the steady decrease in global order as the system is extended. Local order and global disorder, along with the complex defect patterns this picture implies, can be seen in a ‘‘snapshot’’ of the particle configuration at $\dot{\gamma}=2.00$ and $N_x=120$ in Fig. 8.

V. DISCUSSION

The steady decrease of the global string correlation in the shearing 2D liquid with a profile biased thermostat is an



FIG. 8. Instantaneous particle configurations from the steady state at $\dot{\gamma}=2$ for cell dimensions $(N_x, N_y)=(120, 16)$. A complex arrangement of ordered string domains and interceding grain boundaries are evident.

important sort of result. *If* the trend persisted for increasingly larger systems and for higher shear rates, it would imply that the shear-induced string phase would not be observed in the thermodynamic limit and, hence, is simply an artifact of the computational machinery. Furthermore, this conclusion would have been reached *independently of the choice of thermostat*. This would mean that presence or absence of the string phase is irrelevant to the important question of criteria for establishing thermostat “correctness.” A thermostat which manages to remove an artifact generated by a finite size effect may well be doing so by means of introducing an artifact of its own [21].

The existence of a short ranged string order, on the other hand, is free of any explicit taint of artifact. The persistence of this local structure in the face of diminishing global structure is an interesting observation. We are unaware of reports of any analogous shear-induced ordering in the form of domains. The lack of size dependence in the shear stress suggests that the stress depends more on the local environment of the particle than on the coherence of global order in the flow direction. We make the tentative suggestion here that this local shear-induced order reflects the specific correlations of the 2D liquid. Unlike the 3D liquid, the equilibrium fluctuations in dense liquids of disks in 2D are characterized by large transient crystal domains. These have been observed experimentally by means of cross photon correlation spectroscopy [22]. It is possible that the local “strings” reported here are the shear-aligned and distorted remnants of these equilibrium fluctuations. The zeroth order version of this proposal would predict that the minimum extent of the string domains in the shearing liquid would equal the equilibrium

correlation length and that the observed onset of “the string phase” corresponds to the shear rate at which the domain extends across the simulation cell. More detailed studies of the dependence of the extent of local correlations on shear rate would help resolve this question.

What is the connection between box length and global structural stability? In the case of shear-induced ordering in 3D, we [3] have reported results which support the suggestion that order is stabilized by pseudo-oscillations in the shear flow which result from applying a steady shear through the periodic boundaries of the simulation box. However, given the independence of I_{lay} with respect to the box length found in the 2D system, this explanation seems unlikely in this case. Instead, our results indicate that the global order is the result of a simulation cell dimension being of the same order as the correlation length among the ordered domains. Increasing the cell length increases the number of uncorrelated domains and so diminishes the global order.

The question of how a domain structure can be maintained under shear is intriguing. The action of the shear on a domain of stringlike order is to convect strings through the grain boundary between domains. The resulting local distortions would be expected to contribute to the shear stress. The degree to which such flow *disrupts* local order versus *establishing* global order is a central issue for this interesting type of dynamics, as well as related phenomena such as the rheology of lamellar phases. As the convection of strings between weakly correlated domains implies local deviations from linear shear flow, the choice of thermostat would be expected to significantly influence the resulting flow.

-
- [1] D. J. Evans and G. P. Morriss, *Statistical Mechanics of Non-equilibrium Liquids* (Academic, London, 1990).
- [2] S. Butler and P. Harrowell, *J. Chem. Phys.* **103**, 4653 (1995).
- [3] S. Butler and P. Harrowell, *J. Chem. Phys.* (to be published).
- [4] D. J. Evans and G. P. Morriss, *Phys. Rev. Lett.* **56**, 2172 (1986).
- [5] M. J. Stevens, M. O. Robbins, and J. F. Belak, *Phys. Rev. Lett.* **66**, 3004 (1991).
- [6] W. Loose and S. Hess, *Rheol. Acta* **28**, 91 (1989).
- [7] A. A. Rigos and G. Wilemski, *J. Phys. Chem.* **96**, 3981 (1992).
- [8] G. Bossis and J. F. Brady, *J. Chem. Phys.* **80**, 5141 (1984).
- [9] G. Bossis, J. F. Brady, and C. Mathis, *J. Coll. Inter. Sci.* **126**, 1 (1988).
- [10] T. Phung and J. F. Brady, in *Slow Dynamics in Condensed Matter*, edited by K. Kawasaki, M. Tokuyama, and T. Kawakatsu, AIP Conf. Proc. No. 256 (AIP, New York, 1992).
- [11] L. V. Woodcock, *Phys. Rev. Lett.* **54**, 1513 (1985).
- [12] D. M. Heyes, *Mol. Phys.* **57**, 1265 (1986).
- [13] B. J. Ackerson, *J. Rheol.* **34**, 553 (1990).
- [14] H. Komatsugawa and S. Nosé, *Phys. Rev. E* **51**, 5944 (1995).
- [15] D. J. Evans, S. T. Cui, H. J. M. Hanley, and G. C. Straty, *Phys. Rev. A* **46**, 6731 (1992).
- [16] D. J. Evans and G. P. Morriss, *Phys. Rev. A* **30**, 1528 (1984).
- [17] Q. W. Lees and S. F. Edwards, *J. Phys. C* **5**, 1921 (1972).
- [18] W. G. Hoover, A. J. C. Ladd, and B. Moran, *Phys. Rev. Lett.* **48**, 1818 (1982).
- [19] D. J. Evans, *J. Chem. Phys.* **78**, 3297 (1983).
- [20] K. Bagchi, H. C. Andersen, and W. Swope, *Phys. Rev. Lett.* **76**, 255 (1996).
- [21] In order to relax the constraint on the streaming velocity, the various profile unbiased thermostats increase the number of degrees of freedom deemed to be *streaming*. As these degrees of freedom are not directly thermostated, the total kinetic energy of the shearing liquid will be *larger* for a PUT than for a PBT at the same “temperature” (defined by the average kinetic energy of the *peculiar* degrees of freedom). This feature alone may explain why ordering is less likely in PUT simulations.
- [22] B. J. Ackerson, T. W. Thomas, and N. A. Clark, *Phys. Rev. A* **31**, 3183 (1985).